

## Article

# Energy Analysis of an Integrated Plant: Fluidized Bed Steam Gasification of Hydrothermally Treated Biomass Coupled to Solid Oxide Fuel Cells

Alessandro Antonio Papa <sup>1,\*</sup>, Andrea Di Carlo <sup>1</sup>, Enrico Bocci <sup>2</sup>, Luca Taglieri <sup>1</sup>, Luca Del Zotto <sup>3</sup>  
and Alberto Gallifuoco <sup>1</sup>

<sup>1</sup> Department of Industrial and Information Engineering & Economics, University of L'Aquila, Via G. Gronchi, 67100 L'Aquila, Italy; andrea.dicarlo1@univaq.it (A.D.C.); luca.taglieri@univaq.it (L.T.); alberto.gallifuoco@univaq.it (A.G.)

<sup>2</sup> Department of Engineering Science (DSI), Marconi University, Via Plinio 44, 00193 Rome, Italy; e.bocci@lab.unimarconi.it

<sup>3</sup> Centro di Ricerca su Energia Ambiente e Territorio—CREAT, Faculty of Engineering of Università eCampus, 22060 Novedrate, Italy; luca.delzotto@unicampus.it

\* Correspondence: alessandroantonio.papa@univaq.it

**Abstract:** An innovative process based on hydrothermal carbonization, gasification, and solid oxide fuel cells (SOFCs) technologies was developed using a commercial process simulation software called ASPEN Plus. The object of this work is to study plant efficiency under various operating conditions. The hydrothermal pre-treatment (HTC) at 200 and 250 °C was modelled as a black box based on the experimental results. The gasifier was modelled as a single reactor vessel with both the fluidized bed steam gasification of solid fuel and the hot gas cleaning system. The SOFC was modelled as a simple grey box with the ASPEN Plus blocks. The effect of HTC temperature and steam/carbon (S/C) ratio on the syngas composition and yield and plant efficiency was studied. The results show that the gasification of hydrochar obtained at 200 °C with S/C ratio of 0.6 gives the best results, namely an energy output of SOFC equal to 1.81 kW/kg<sub>Biomass</sub>, and overall process efficiency of 36%.

**Keywords:** biomass gasification; SOFC; hydrothermal carbonization; ASPEN Plus; energy analysis



**Citation:** Papa, A.A.; Di Carlo, A.; Bocci, E.; Taglieri, L.; Del Zotto, L.; Gallifuoco, A. Energy Analysis of an Integrated Plant: Fluidized Bed Steam Gasification of Hydrothermally Treated Biomass Coupled to Solid Oxide Fuel Cells. *Energies* **2021**, *14*, 7331. <https://doi.org/10.3390/en14217331>

Academic Editor: Dino Musmarra

Received: 8 September 2021

Accepted: 29 October 2021

Published: 4 November 2021

**Publisher's Note:** MDPI stays neutral with regard to jurisdictional claims in published maps and institutional affiliations.



**Copyright:** © 2021 by the authors. Licensee MDPI, Basel, Switzerland. This article is an open access article distributed under the terms and conditions of the Creative Commons Attribution (CC BY) license (<https://creativecommons.org/licenses/by/4.0/>).

## 1. Introduction

The challenges related to global warming, national energy security, and dependency has brought the need for alternatives to fossil fuels. Biomass is one of the preferable renewable energy sources, the third-largest in the world after coal and oil [1].

Gasification is considered a very efficient technology for the thermo-chemical conversion of biomass, becoming one of the preferable ways to exploit solid waste. In particular, steam gasification of biomass in a dual fluidized bed reactors can produce gas with a high concentration of H<sub>2</sub> and high lower heating value (LHV) [2], which can be used to produce electrical power by conventional devices such as internal combustion engines (ICE). However, efficient and clean energy conversion devices must be developed and assessed, especially in the low-medium power range. High-temperature fuel cells (such as SOFC) represent the most promising technologies for achieving these results [3]. The operating temperatures of biomass gasification plants and SOFCs match perfectly. In the last few years, many studies have been carried out to determine the optimal operating conditions, the performance, and the potentials and limitations of various integrated power plant coupling gasifier and SOFC [4–16].

In the work of Toonsenn et al. [4] the influence of gasification technology, gas cleaning technology, and system scale on the overall system performance of integrated solid oxide fuel cell-gas turbine (SOFC-GT) and biomass gasification systems were evaluated. In

particular, four energy systems have been investigated using the thermodynamic flow-sheeting program 'Cycle-Tempo'. The results of this study show that the highest electrical exergy efficiency of 49.9% is obtained with air gasification and high temperature gas cleaning at large-scale system. Athanasiou et al. [5,16] carried out a thermodynamic analysis of an integrated process composed of downdraft gasifier, SOFCs, and turbine. Experimental data have been obtained for olive kernels gasification. The overall electrical efficiency can, ideally, reach 62%. In the work of Cordiner et al. [6], a 14 kW integrated SOFC-gasifier system has been studied to address the effect of the gasifier operating conditions on fuel cell performance. An equilibrium model has been used to simulate the gasification process, whereas a 3D fluid dynamics simulation (FLUENT) coupled with an external model for the electrochemical reactions has been used to predict the fuel cell performance. The efficiency of the system is 45.8%. Panopoulos et al. [7,8] investigated a small scale combined heat and power system with an allothermal gasifier and SOFC using Aspen Plus™ process simulation software. The system is based on the "Biomass Heat Pipe Reformer" (BioHPR), wherein the heat transfer between the combustor and the gasifier is obtained by high temperature heat pipes. The results showed that the system can produce 140 kW<sub>e</sub> with a global electrical efficiency of 36% and Fuel Utilization in the SOFC equal to 0.7. Zhao et al. [9] also modeled a SOFC–GT power plant. MATLAB was used to develop an optimization algorithm to predict the performance characteristics of hybrid systems sizing from 2000 to 2500 W m<sup>-2</sup>. Energy and entropy balance analysis has been carried out to observe the irreversibility distribution within the plant and the contribution of different components. The analysis was useful to determine better integration strategies for advanced SOFC–GT systems. Nagel et al. [10] developed a Biomass Integrated Gasifier and Fuel Cell System (B-IGFC) concept feeding the SOFC with fuel gas from an updraft gasification of wood. During a long-term test, the gasifier and the catalytic partial oxidation operated without problems, producing gas with relatively constant properties to deliver to the SOFC system. The results showed that the SOFC produced 40% less current compared to methane operation. The process conditions prevent carbon deposition. Ash deposits have been identified as the main obstacle to smooth operation of the SOFC. Baron et al. [11] tested a CGO-based IT-SOFC (intermediate temperature solid oxide fuel cell with a 60:40 wt.% Ni:CGO-10 (Ce<sub>0.9</sub>Gd<sub>0.1</sub>O<sub>1.95</sub>) cermet as anode material) in moist hydrogen/nitrogen mixtures and in various emulated gasification mixtures at 650 °C. The results showed that the CO decreased the performance of the anode compared to H<sub>2</sub>. CO<sub>2</sub> did not affect cell performance, whilst methane (5 and 10%) decreased the performance due to carbon deposition. Di Carlo et al. [12] carried out a numerical analysis of a SOFC/mGT and biomass gasification system by using ChemCAD software. The gasifier model was developed, and tar evolution was studied. The results shown that the wood-gas obtained was rich in H<sub>2</sub> and CO and almost no tar content. A sensitivity analysis was conducted to find the optimal operation condition. The totally efficiency of the system ranged between 36 and 44%. The best results were obtained by increasing the cell temperature at 800 °C, leading to a power produced improvement of 22%. Pieratti et al. [13] have set up a continuous small-scale steam gasification system (fixed bed) to obtain syngas suitable for fuel cell. The results showed that tar and H<sub>2</sub>S represent the main critical issues, rapidly decreasing the life of the SOFC. The efficiency of the cell, during a test with a stack of 24 cells coupled with the gasifier, has been assessed at 40%. Liu et al. [14] evaluated by thermodynamic calculations the performance of a commercial 5 kW SOFC CHP system (Alpha unit from Siemens-FCT) coupled with a downdraft fixed-bed gasifier. In particular, the effects of high and low temperature gas cleaning have been investigated (HTGCS and CTGCS, respectively). The results show no significant differences of the electrical efficiency between the two types of gas cleaning system (21.6% with HTGCS and 23.1% with CTGCS), whereas the high temperature offers higher heat efficiency (44.4%). Omosun et al. [15] also studied the effect of cold and hot gas cleaning process. A steady-state model of the integrated system of SOFC and fixed bed gasifier for power and heat production was developed in the gPROMS modelling tool. For the two options, the operating temperature

of the gasifier is assumed to be 600 °C e 900 °C for hot and cold gas cleaning, respectively. The system was studied in terms of efficiency and for cost analysis. The results shown that both electrical and system efficiency is higher with the hot process. The critical aspects of using biomass gasification with SOFC remain the tar and detrimental trace elements (such as H<sub>2</sub>S) produced by the gasification process. The tolerance limits of the SOFC are among the lowest [17]. Thus, several hot gas cleaning and conditioning systems have been proposed [18]: one of the most promising technologies is developed in the UNIQUE concept [19]. A bundle of catalytic filter candles is inserted in the freeboard of a fluidized bed gasifier to convert and reduce tars in the product gas. In any case, efficacious tar and sulfur concentration must be low yet in the raw gas from the gasifier. This requirement nullifies the great potential of the gasification technology since most of the organic waste is not exploitable unless pre-treatments are carried out on the solid fuel feedstock. Several pre-treatment process to obtain a coal-like material from biowaste have been suggested, and hydrothermal carbonization (HTC) is one of them. Hydrothermal carbonization is an artificial coalification process in hot pressurized water between 175 °C and 250 °C.

During HTC, the biomass undergoes a complex network of reactions that produce a carbon-rich, solid hydrochar (HC), a liquid phase with dissolved organic compounds and a relatively small amount of gas. The process raises the higher heating value (HHV) of the biomass, reduces the H/C and O/C ratio [20], and improves its mechanical properties (such as grindability). The properties of HC are comparable to those of lignite [21]. HTC increases the energy density of the feedstock, which is beneficial to the logistics of biomass use. Finally, in the last few years, hydrothermal conversions attracted interest for producing value-added products [22].

Differently from torrefaction and pyrolysis, HTC is suitable for the use of high moisture biomass. The reactions proceed to destroy the structure of the biomass and to make it more hydrophobic, facilitating mechanical dewatering and reducing the energy demand of the thermal drying. Ramke demonstrated that 57–68% dry matter contents could be achieved with laboratory presses for hydrochar from organic waste [23]. Hwang et al. [24] shown that the HTC from municipal solid waste (MSW) could produce hydrochar with minimal carbon loss without a drying process. Zhao et al. reported that the energy consumption of this process was only about 22% of that consumed in the conventional thermal drying [25]. Prawisudha et al. [26] further reported that the volume-based energy density of hydrochars was approximately four to five times higher than that of the raw MSW on a dry basis.

Lee et al. [27] carried out air gasification experiments on hydrochar produced by HTC of sewage sludge. The results demonstrated that the product gas increased its LHV by 0.98 MJ/Nm<sup>3</sup> and cold gas efficiency by 5.8% more, compared to the product gas obtained by the gasification of the non-treated feedstock. Furthermore, the hydrothermally treated sludge cake generates less tar during the gasification than the raw sludge cake. The total tar and naphthalene reduced by 28% and 78%, respectively. A further advantage of the HTC pretreatment would be reducing the sulfur and nitrogen content in the feedstock, which are precursors of gaseous contaminants as the reaction temperature rises.

Many biomass feedstocks, including wood, straw, cut grass, municipal waste, digestate from anaerobic digestion, distiller's grains, microalgae, and bark mulch have been successfully carbonized with HTC in laboratory-scale experiments [28,29]. The degree of carbonization depends on the reaction temperature and residence time. The higher the temperatures and residence times, the higher the carbon content and calorific value and the lower mass and energy yields [30]. Besides hydrochar, HTC produces water, CO<sub>2</sub>, small amounts of CO, H<sub>2</sub> and hydrocarbons, and dissolved organic and inorganic compounds. Gerhardt, Berg and Kamm identified acetic acid, formic acid, glycolic acid, levulinic acid, phenol, furfural, HMF, and sugars in the aqueous phase using HPLC analysis [31]. Most of them are also valuable platform chemicals for green syntheses [32].

This work aims to assess the integration and the performances of a system composed by:

1. An HTC section for the pre-treatment of wet biomass;

2. A dual fluidized bed gasifier using the hydrochar for the production of a rich hydrogen gas with hot gas cleaning and conditioning integrated into the same reactor vessel (UNIQUE concept [19]);
3. A SOFC section for exploiting the product gas to produce electricity.

The system is evaluated thermodynamically through Aspen plus simulations V 11 (37.0.0.395). The HTC model was developed using the experimental results obtained at laboratory scale, using silver fir sawdust as biomass feedstock at two different HTC temperatures, 200 and 250 °C [33]. The remaining section of the system have been simulated using Aspen plus components. Finally, the results obtained for the hydrochars have been compared with those of the non-pretreated biomass. The inorganic syngas contaminants detrimental to the SOFC have been neglected, this being out of scope of this work (that is, to analyze HTC temperature and steam/carbon (S/C) ratio on the syngas composition and yield and overall plant efficiency that are not affected by contaminants).

## 2. Modelling

The simulation of an industrial plant for the exploitation of biomass and the energy analysis went according to the following. All physical properties of the conventional components ( $H_2$ ,  $CO$ ,  $CH_4$ ,  $H_2O$  . . . ) were estimated by the Peng-Robinson state equation model. Biomass and hydrochars from the HTC are characterized by their ultimate and proximate analyses and not by their chemical formula as they are classified as non-conventional solids. The tools HCOALGEN and DCOALIG have been used to calculate the lower heating value (LHV), formation enthalpy (HCOALGEN) and density (DCOALIG) of the biomass. The data for these calculations for the hydrochar (proximate analyses, ultimate analyses, and sulfur analyses) have been taken from the previous work of Gallifuoco et al. [33]. Figure 1 shows the block diagram of the process.

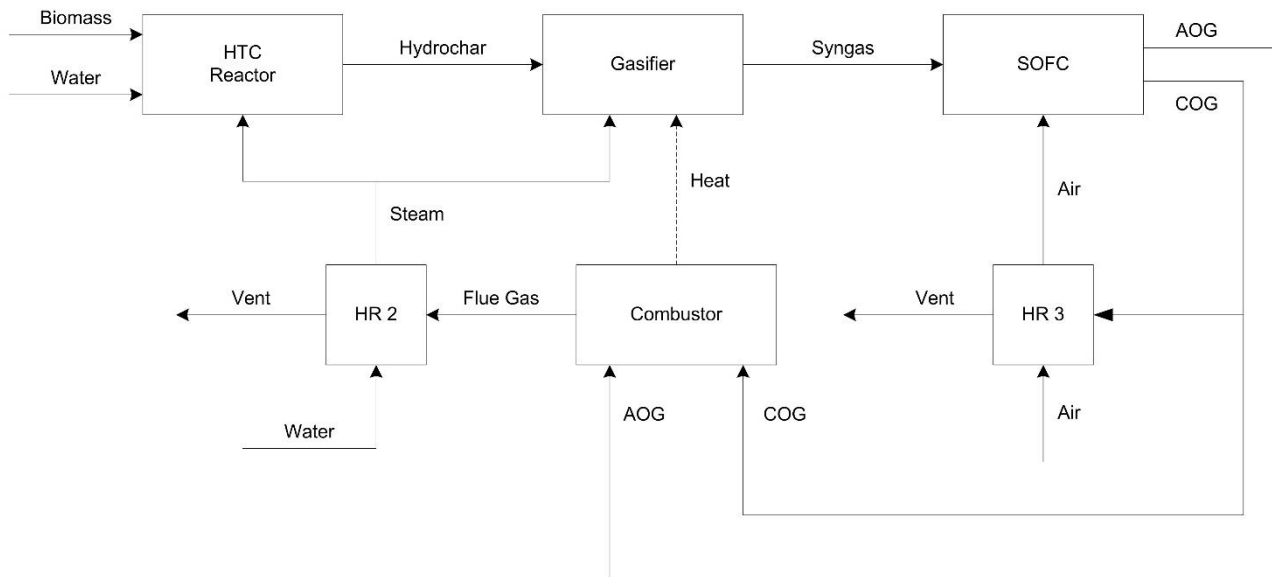


**Figure 1.** Block diagram of the process (AOG: anode off gas; COG: cathode off gas; HR: heat recovery).

The power plant includes three sections: hydrothermal carbonization (HTC), gasification (GAS), and SOFC (see Figure 2). A plant without the HTC section, thus where B, Biomass, enter as HCDRY in Figure 2, has been also considered to compare the plant efficiency with and without HTC. Table 1 reports a description of the main Aspen blocks used in the model.

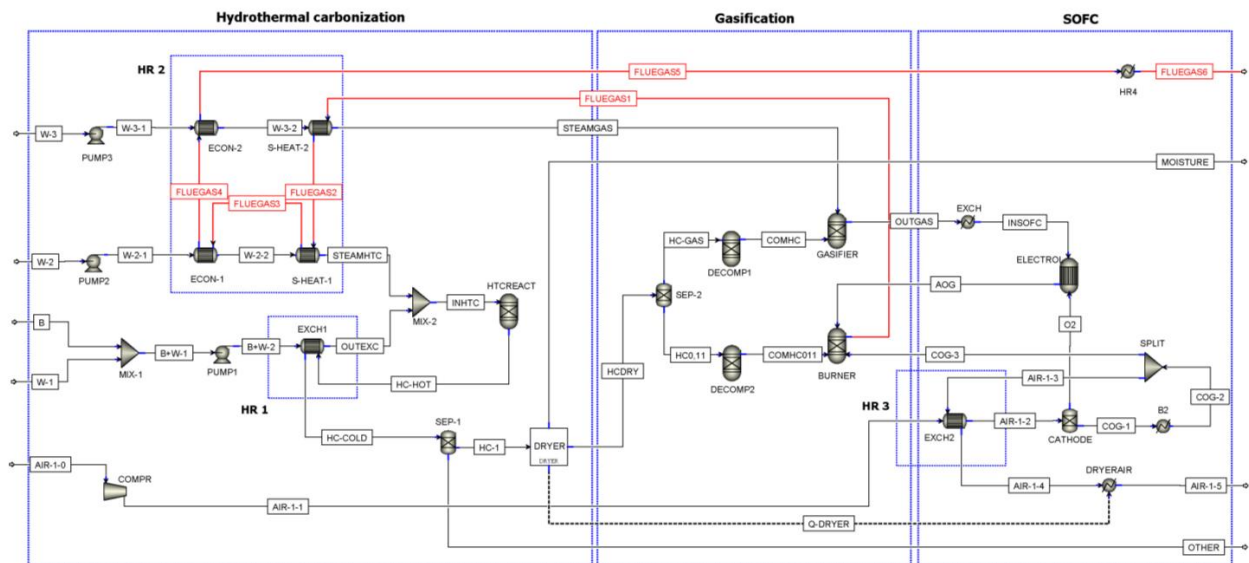


Figure 2. Flowsheet of the process (ECON: Economizer; S-HEAT: Superheater).

Table 1. Description of ASPEN Plus flowsheet unit operation presented in Figure 2.

ASPEN Plus Name	Block ID	Description
RYIELD	DECOMP-1	The reactor converts the non-conventional stream “Hydrochar” into its conventional components The reactor simulates partial oxidation and gasification and restricted chemical equilibrium of the specified reactions to set the syngas composition by specifying a temperature approach for individual reactions
	DECOMP-2	
RGIBBS	GASIFIER	The reactor simulates the oxidation of the conventional components of hydrochar The reactor simulates the anode of the SOFC
	BURNER	
SEP	ELECTROL	Separator simulates a filter press used to reduce the water content of the hydrochar
	SEP-1	Separator separates the hydrochar unreacted (HC0,11) from the hydrochar to gasifier (WETHC)
	SEP-2	

### 2.1. HTC Model

The HTC is modelled as a black box using data of the laboratory experiments performed in a stainless-steel batch reactor with an internal volume of 200 mL (further details about experimental apparatus and procedure are reported in previous works [30,33]).

The tests were conducted at two reaction temperatures ( $T = 200$  and  $250$  °C, labelled HTC-200 and HTC-250, respectively), residence time 30 min and water to dry biomass ratio 7:1.

Solid, liquid, and gas yields have been calculated according to Equations (1)–(3) to perform the mass balances of the process:

$$Y_{HC} = m_{HC,dry} / m_{Biomass,dry} \cdot 100 \quad (1)$$

$$Y_{gas} = m_{gas,dry} / m_{Biomass,dry} \cdot 100 \quad (2)$$

$$Y_{Liquid\ phase} = 100 - Y_{HC} - Y_{gas} \quad (3)$$

where  $m_{HC,dry}$  and  $m_{gas,dry}$  are the mass of the dry hydrochar and gas produced, respectively, and  $m_{Biomass,dry}$  is the mass of the treated dry biomass.

The following assumptions allow for assessing the ash and C, H, N, S, and O elemental mass balances:

- The feedstock is fed dry. The moisture is considered adding liquid water.
- CO<sub>2</sub> is the only gaseous product. Indeed, other gases represent a very small fraction that can be neglected without affecting the goodness of the results obtained from the simulations [34,35].
- The estimate of organic and inorganic compounds dissolved in the liquid phase is determined by the difference between the CHNSO and ash content of the feedstock and those recovered in the hydrochar and gas phase.
- The organic compounds are lumped as organic acid (acetic, formic, lactic, levulinic, and propionic) and furfural, according to the main findings reported in the literature [36,37].
- Biomass and hydrochar are defined as a nonconventional stream based on their proximate and ultimate analyses. Aspen Plus always assigns substreams of type NC to nonconventional solids (i.e., nonconventional solids are coal and wood pulp) [38].

## 2.2. Gasification Model

The simulated gasifier is based on the UNIQUE concept [19], consisting of a compact gasifier that integrates into a single reactor vessel both the fluidized bed steam gasification of solid fuel and the hot gas cleaning system, employing a bundle of ceramic filter candles operating at high temperature (800–850 °C) in the gasifier freeboard. Experiments by Rapagnà et al. [39] and Savuto et al. [40] demonstrated that tars could be almost wholly reformed due to the catalytic filter candles and methane steam reforming is close to equilibrium. For this reason, a Gibbs reactor was considered the proper one to model the gas reactions occurring in the freeboard of the gasifier with a catalytic filter candle.

In dual fluidized bed steam gasifiers, about 10–11% of the char produced by the pyrolysis of the fuel remain as unconverted due to the kinetic and mass transport limitations [41]. Consequently, not all of the char is converted into product gas, and the unconverted can be fed to the combustor to supply the heat required by the gasification process. In the modelling subsection, 10% of the feeding dry hydrochar is split and sent to the burner subsection. The remaining hydrochar goes to the steam gasifier section. Subsequently, the hydrochar material is transformed from a non-conventional solid into its elements in the two RYIELDs (DECOMP1 and DECOMP2). This practice is common when dealing with solid fuel materials in Aspen Plus. The individual products yield of the R-Yield blocks were estimated using a calculator block, a Fortran subroutine that computes the products yields of the decomposition based on the hydrochar ultimate and proximate analysis. The two streams from the DECOMPs feed the two GIBBS reactors to simulate the complete combustion of the char and of the additional fuel with air, and the gasification with steam. For the gasification process in the R-Gibbs reactor, the option “temperature approach” for the steam methane reforming reaction was adopted to obtain a methane content in the product gas that is not close to zero as should be, by thermodynamics, at such high operating temperature (800–850 °C).

The literature lacks information on hydrochar processing in steam gasifiers with catalytic ceramic candles in the freeboard. Accordingly, the model was tuned and validated using data available for biomass [39,40] at two different steam to biomass ratio (0.5 and 1) and at 800 °C. A temperature approach of –100 °C was selected for the steam reforming of methane. The results are reported in Figure 3, which shown that the model predicts the experimental results satisfactorily. Indeed, increasing the S/B ratio more hydrogen and less CO is obtained due to the water gas shift reaction (WGS).

## 2.3. SOFC Model

The SOFC modelling is based on a simplified grey box model previously validated [42]. The assumptions of this model are:

- The reactions inside the cell are stoichiometric combustion at  $T = 740$  °C, and an equilibrium reactor RGibbs (ELECTROL) is used.
- Fuel utilization has been varied to obtain enough fuel residue gas (AOG) from the SOFC to be used in the gasification process, thus avoiding the need for additional fuel.

- The SOFC block is assumed isothermal. The heat duty of the combustion reaction is consumed to produce electricity (electrical efficiency set to 0.5 [43]), and the rest is transferred to the cathode stream.
- Consequently, the mass flow rate of air to the cathode has been varied to dispose of the excess of heat.

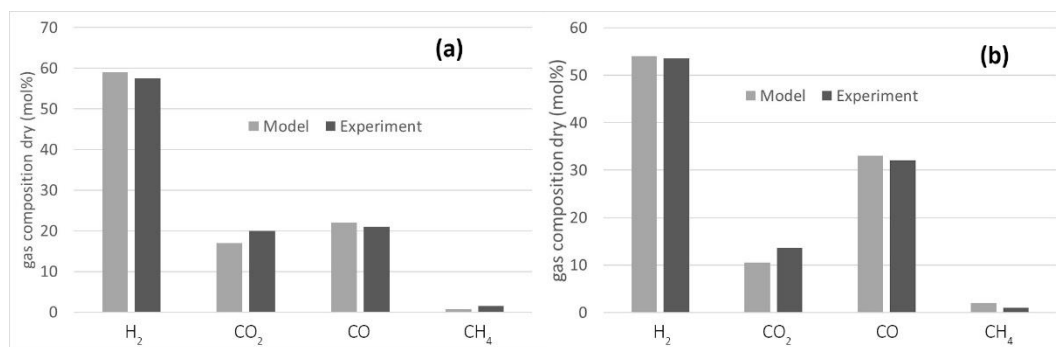


**Figure 3.** Comparison of the gasifier model with the experimental results for steam gasification of biomass: (a) S/B = 1 [39]; (b) S/B = 0.5 [40].

#### 2.4. Process Design

1 kg/h of biomass (B) is mixed with water (W-1). The pump raises the pressure to feed the mixture to the HTC reactor. The heat exchanger preheats the slurry (HR1). The superheated steam is added to the mixture to attain the process temperature and ensure the desired water/biomass ratio. The hydrochar and the aqueous products are recovered from the bottom of the reactor and recirculate in Exch-1. A filter press separates solid and liquid products, and the hydrochar is dried.

Dry hydrochar is feed to the gasification section. The flow rate of steam has been calculated as a function of the selected steam to fuel parameter. The syngas (OUTGAS) composition is determined using a Gibbs reactor with a temperature approach limited to steam methane reforming (Section 2.2).

The burner (BURN-1) is fed with 11% hydrochar and possibly with additional fuel to obtain the heat duty of blocks GAS, DECOMP-1, and DECOMP-2. The flue gases are utilized to produce the steam needed in the HTC and gasification sections (HR2).

Syngas and air are fed to the SOFC. Fuel utilization factor and mass flow rate of air are determined using *Design Specs* based on model's assumption (see Section 2.3). CATHODE, simulated as a separator, allow feeding the needed air (based on the fuel utilization factor) at the SOFC.

The Cathode Off Gas (stream COG), still rich in oxygen, is recirculated to preheat the air before the SOFC (HR3) and the burner block.

The effects of hydrothermal carbonization temperature and steam/carbon ratio in the gasification section are evaluated on the plant performances. Table 1 reports the operating conditions used in the modelling.

The overall process efficiency is calculated by:

$$\eta = \frac{E_{SOFC} - E_{cons}}{\dot{m}_{bio}LHV + E_{th}} \quad (4)$$

where  $E_{SOFC}$  is the electric power produced by the SOFC,  $E_{cons}$  is the electric power demand,  $\dot{m}_{bio}$  is the mass flow rate of biomass multiplied,  $LHV$  is the low heating value, and  $E_{th}$  is the additional thermal power required by the process.

The electric power demand ( $E_{cons}$ ) includes the required energy for the pumps and the compressor. Pumps 1 and 2 have to ensure the pressure to the reactor (experimental data) and compensate the pressure drop in heat exchangers (conservatively assumed to be equal to 3 bar each). Pump 3 feeds the water to the gasifier section, the rise in pressure

required is assumed equal to 2 bar. The overall pump efficiency is set to 0.5 [44]. The compressor supplies the air to the SOFC and burner section. The increment in pressure and the efficiency is set to 200 mbar and 0.75, respectively [44].

### 3. Results and Discussion

Table 2 shows the gasifier output composition at the different operating conditions adopted.

**Table 2.** Operating conditions.

Hydrothermal Carbonization	
T [°C]	200–250
p [bar]	18–48
Water/Biomass	7
Gasification	
T [°C]	800
Steam/Carbon	0.6–1–1.4
SOFC	
T [°C]	740

High S/C ratios increases the production of H<sub>2</sub> and CO<sub>2</sub> and decrease CO and CH<sub>4</sub> concentrations. These results indicate that a higher S/C ratio enhances water gas, steam methane, and WGS reactions.

Findings on the effect of HTC temperature on syngas composition are in line with that of [45]. Higher HTC temperature reduces volatile matter content and increase the fixed carbon influencing the syngas production in terms of composition and gas yield. Hydrochars' carbon content increases with temperature, increasing the availability of char for gasification, while the lower O/C ratio enhanced the concentration of CO and CH<sub>4</sub>. Hydrogen content is almost the same in all simulations, with the evolution more affected by the S/C ratio. The higher variation of gas composition was obtained for S/C = 1. In particular, the H<sub>2</sub> concentration varied less than 7%, while CO, CO<sub>2</sub>, and CH<sub>4</sub> shown a significantly effect (+24.7%, −42.6%, and +136.8%, respectively).

The higher the temperature of HTC, the higher the yield of gas. However, the lower hydrochar yield at 250 °C leads to decreased gas production (up to −38%). This consequence also affects the energy output by the SOFC and then the overall efficiency of the process. Figure 4 shows the effect of the S/C ratio and HTC temperature on the overall process efficiency. In order to show the effect of the HTC pretreatment, the overall process efficiency was calculated also starting from the raw dry biomass without HTC (named Biomass in the Figure 4). The highest efficiency occurs with hydrochar produced at 200 °C, comparable to that of biomass. Furthermore, the overall process efficiency ( $\eta$ ) shows a decreasing trend with the S/C ratio.

As reported in the literature, the electrical efficiency of the SOFC ranges from 30 to 40% depending by efficiency and fuel utilization factor, both for steam gasification [8,12] and gasification with air [5,16]. The value obtained with raw biomass is quite similar, confirming the goodness of the model.

The lower  $\eta$  value is obtained with HTC-250 and S/C equal to 0.6, due to the incomplete conversion of HC in the gasification step, as discussed above (see Table 2).

The results refer to the dry biomass input, neglecting the energy required for the drying phase. It is worth noting that a wet feed reduces the efficiency of gasification of the raw biomass while it does not affect the efficiency of the process with HTC pretreatment.

Furthermore, although out of scope of this paper, it is worth pointing out that HTC process reduces the contaminant content of biomass. During the process the reactions of dehydration, dechlorination, denitrification, and coalification take place improving fuel properties of the treated substrates [46]. Hydrochars generally exhibit higher heating

values, higher ash fusion temperatures, and reduced sulfur, chlorine, and nitrogen contents compared to the raw biomass [27,47,48]. Also, if the volatile matter content is reduced, then the produced syngas could have less tar [45]. Figure 5 reports the percentage of the thermal energy demand of the HTC, gasification, and SOFC sections to the total thermal energy demand. These energy requests would be necessary to heat the streams at the inlet of each section if there would not be any heat recovery. The simulation with HTC-250 gave the lower SOFC and gasification energy requests, and the higher HTC energy request. As expected, the contribution of SOFC and gasification increase as a function of the S/C ratio.

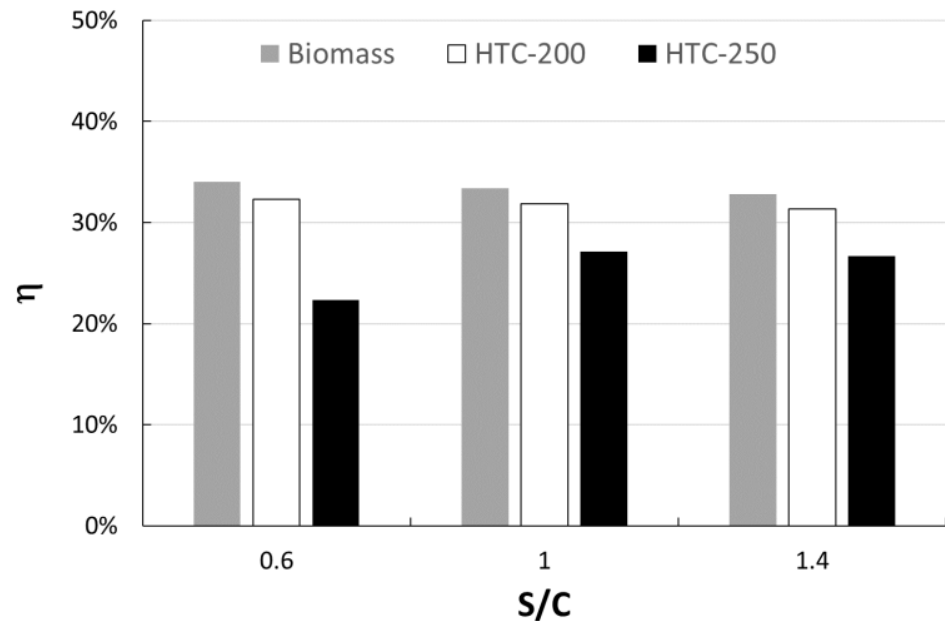


Figure 4. Process efficiency as a function of S/C ratio.

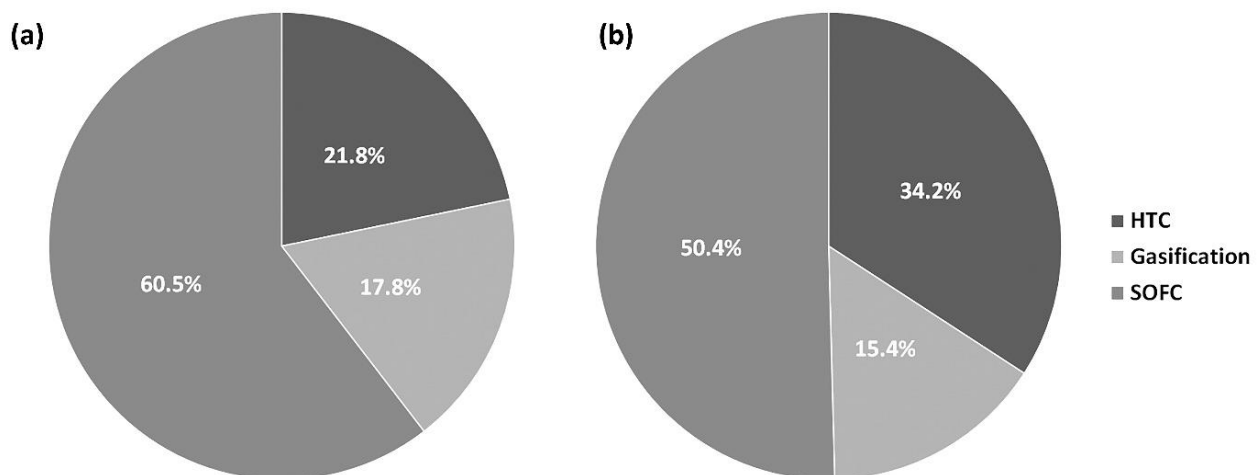


Figure 5. Distribution of thermal energy demand (S/C = 0.6): (a) HTC-200; (b) HTC-250.

To enhance the efficiency of the process, the present process plant model aims to promote heat recovery. The HR1 allow to preheat the slurry (biomass/water) up to 170 and 220 °C (in the simulation with HTC-200 and 250 respectively) using the mixture of hydrochar, water, and organic compounds from the HTC reactor. In HR2, the flue gas from the burner is used to produce the steam requested by the HTC and gasification reactors. The COG is used to preheat the air fed to the SOFC at 550 °C (HR3).

Furthermore, the AOG is used to replace the auxiliary fuel in the gasification section. The fuel utilization parameter of the SOFC is calculated as described in Section 2.4. The results showed that the fuel utilization varied from 78.5% to 87.5% (see Table 3).

**Table 3.** Gasifier output: syngas composition, gas yield and residual carbon as function of S/C Ratio.

S/C Ratio	HTC-200			HTC-250		
	0.6	1	1.4	0.6	1	1.4
H <sub>2</sub> O (%wet mole fraction)	4.1%	9.7%	15.5%	2.5%	4.2%	9.8%
CO <sub>2</sub> (%wet mole fraction)	4.4%	7.5%	9.7%	3.0%	4.3%	7.4%
H <sub>2</sub> (%wet mole fraction)	43.3%	47.1%	47.0%	41.2%	44.1%	47.7%
CO (%wet mole fraction)	41.5%	32.7%	26.2%	43.5%	40.7%	32.2%
CH <sub>4</sub> (%wet mole fraction)	6.5%	2.8%	1.4%	9.4%	6.5%	2.8%
C residue (kg/kg <sub>HC</sub> )	-	-	-	0.11	-	-
Gas yield (Nm <sup>3</sup> /kg <sub>HC</sub> )	1.54	1.88	2.16	1.45	1.97	2.40
Gas yield (Nm <sup>3</sup> /kg <sub>Biomass</sub> )	1.31	1.60	1.84	0.81	1.10	1.34

A lower fuel utilization value indicates that the required energy for the gasification step is high, then a fraction of the output gas from the gasifier must be recirculated, reducing the electrical energy output. The higher value of the fuel utilization parameter is obtained with HTC-250 (S/C = 0.6) due to the incomplete gasification of hydrochar. The amount of non-converted char recirculated to the burner is higher in this last case so that less additional fuel is required.

The fuel utilization is a key parameter of the SOFC, influencing its efficiency and the composition of the AOG. Higher fuel utilization (>85%) causes a loss of SOFC performance, while a low value, although it allows one to work safely, results in low efficiency [9,14].

The results of the SOFC section are reported in Table 4. The data shows that the least FU is obtained with biomass due to the higher energy demand of the gasification step.

**Table 4.** Fuel utilization (FU) and energy produced by the SOFC.

	S/C	FU	Energy Output [kW/kg <sub>Biomass</sub> ]
Biomass	0.6	79.0%	1.90
	1	76.5%	1.87
	1.4	74.8%	1.83
HTC-200	0.6	83.6%	1.81
	1	80.4%	1.79
	1.4	78.5%	1.76
HTC-250	0.6	87.5%	1.27
	1	84.3%	1.54
	1.4	81.1%	1.52

The HTC pretreatment at 200 °C leads to an energy output higher than that obtained with HTC-250. Despite this, HC has a lower sulfur content. This parameter is crucial for the syngas utilization in SOFC due to the meagre concentration limit of H<sub>2</sub>S.

The flue gas and COG outlet conditions are reported in Table 5. The flue gas discharge temperature is always higher than the dew point. As shown in the simulation with HTC-200, the temperature of this stream is relatively high, making it possible for further utilizing. With HTC-200, the output flue gas could be used in ORC.

Mass balances simulated the HTC liquid phase composition as reported in the literature [37]. However, this process output deserves further investigations.

Research is in progress aiming to a more in-depth characterization of this stream, previously studied just as a tool for monitoring the reaction [49], to evaluate the recirculation in the process, reducing the freshwater utilization, and the recovery of high value-added chemicals.

**Table 5.** Synopsis of the outlet condition of flue gas and COG (Flue gas dewpoints calculated from water vapor partial pressure).

S/C		HTC-200			HTC-250		
		0.6	1	1.4	0.6	1	1.4
Flue gas	m [kg/h]	3.7	4.0	4.27	2.5	3.0	3.3
	T [°C]	402	344	288	91	119	85
	Dewpoint [°C]	71	74	76	70	72	74
COG	m [kg/h]	28.6	27.9	27.3	20.1	24.3	23.8
	T [°C]	180	176	173	184	184	180

#### 4. Conclusions

Hydrothermal carbonization, gasification, and SOFC technologies were studied in a combined process to exploit biomass simulated with ASPEN Plus.

HTC conditions affect the syngas yield and composition and the fuel utilization factor of the SOFC. The results showed that concentration of CO and CH<sub>4</sub> increase with HTC process temperature, while the CO<sub>2</sub> decreases. The lower value of fuel utilization is obtained with biomass, while the higher with hydrochar is produced at 250 °C. Lower HTC temperatures lead to the increase of the gas yield, which allows obtaining higher energy output of the SOFC and process efficiency similar to the one obtained without HTC.

Thus, the HTC process at 200 °C seems to be a very effective pretreatment in order to exploit biomass that cannot be gasified as they are. The heat recovery allows avoiding the use of auxiliary fuel to produce steam and for the gasification step. Furthermore, the flue gas discharging temperature is relatively high in the simulation with HTC-200.

**Author Contributions:** Conceptualization, A.A.P., A.G., and A.D.C.; methodology, A.A.P., A.D.C., and E.B.; software, A.A.P.; validation, A.A.P., A.D.C., and L.T.; investigation, A.A.P., A.G., and L.T.; data curation, L.D.Z.; writing—original draft preparation, A.A.P., A.D.C.; writing—review and editing, A.A.P., A.D.C., E.B., L.T., L.D.Z., and A.G.; supervision, A.G.; project administration, E.B.; funding acquisition, A.D.C. and E.B. All authors have read and agreed to the published version of the manuscript.

**Funding:** This research has received funding from the European Union’s Horizon 2020 research and innovation program under grant agreement No 101006656 GICO project.

**Institutional Review Board Statement:** Not applicable.

**Informed Consent Statement:** Not applicable.

**Data Availability Statement:** The data presented in this study are available on request from the corresponding author.

**Conflicts of Interest:** The authors declare no conflict of interest.

#### References

- Pala, L.P.R.; Wang, Q.; Kolb, G.; Hessel, V. Steam Gasification of Biomass with Subsequent Syngas Adjustment Using Shift Reaction for Syngas Production: An Aspen Plus Model. *Renew. Energy* **2017**, *101*, 484–492. [[CrossRef](#)]
- Hofbauer, H.; Veronik, G.; Fleck, T.; Rauch, R.; Mackinger, H.; Fercher, E. The FICFB—Gasification Process. In *Developments in Thermochemical Biomass Conversion: Volume 1/Volume 2*; Bridgwater, A.V., Boocock, D.G.B., Eds.; Springer: Dordrecht, The Netherlands, 1997; pp. 1016–1025, ISBN 978-94-009-1559-6.
- Bocci, E.; Di Carlo, A.; McPhail, S.J.; Gallucci, K.; Foscolo, P.U.; Moneti, M.; Villarini, M.; Carlini, M. Biomass to Fuel Cells State of the Art: A Review of the Most Innovative Technology Solutions. *Int. J. Hydrogen Energy* **2014**, *39*, 21876–21895. [[CrossRef](#)]
- Toonssen, R.; Sollai, S.; Aravind, P.V.; Woudstra, N.; Verkooijen, A.H.M. Alternative System Designs of Biomass Gasification SOFC/GT Hybrid Systems. *Int. J. Hydrogen Energy* **2011**, *36*, 10414–10425. [[CrossRef](#)]
- Athanasiou, C.; Vakouftsi, E.; Coutelieris, F.A.; Marnellos, G.; Zabaniotou, A. Efficiencies of Olive Kernel Gasification Combined Cycle with Solid Oxide Fuel Cells (SOFCs). *Chem. Eng. J.* **2009**, *149*, 183–190. [[CrossRef](#)]
- Cordiner, S.; Feola, M.; Mulone, V.; Romanelli, F. Analysis of a SOFC Energy Generation System Fuelled with Biomass Reformate. *Appl. Therm. Eng.* **2007**, *27*, 738–747. [[CrossRef](#)]

7. Panopoulos, K.D.; Fryda, L.; Karl, J.; Poulou, S.; Kakaras, E. High Temperature Solid Oxide Fuel Cell Integrated with Novel Allothermal Biomass Gasification: Part II: Exergy Analysis. *J. Power Sources* **2006**, *159*, 586–594. [[CrossRef](#)]
8. Panopoulos, K.D.; Fryda, L.E.; Karl, J.; Poulou, S.; Kakaras, E. High Temperature Solid Oxide Fuel Cell Integrated with Novel Allothermal Biomass Gasification: Part I: Modelling and Feasibility Study. *J. Power Sources* **2006**, *159*, 570–585. [[CrossRef](#)]
9. Zhao, Y.; Sadhukhan, J.; Lanzini, A.; Brandon, N.; Shah, N. Optimal Integration Strategies for a Syngas Fuelled SOFC and Gas Turbine Hybrid. *J. Power Sources* **2011**, *196*, 9516–9527. [[CrossRef](#)]
10. Nagel, F.P.; Ghosh, S.; Pitta, C.; Schildhauer, T.J.; Biollaz, S. Biomass Integrated Gasification Fuel Cell Systems—Concept Development and Experimental Results. *Biomass Bioenergy* **2011**, *35*, 354–362. [[CrossRef](#)]
11. Baron, S.; Brandon, N.; Atkinson, A.; Steele, B.; Rudkin, R. The Impact of Wood-Derived Gasification Gases on Ni-CGO Anodes in Intermediate Temperature Solid Oxide Fuel Cells. *J. Power Sources* **2004**, *126*, 58–66. [[CrossRef](#)]
12. Di Carlo, A.; Borello, D.; Bocci, E. Process Simulation of a Hybrid SOFC/MGT and Enriched Air/Steam Fluidized Bed Gasifier Power Plant. *Int. J. Hydrogen Energy* **2013**, *38*, 5857–5874. [[CrossRef](#)]
13. Pieratti, E.; Baratieri, M.; Ceschini, S.; Tognana, L.; Baggio, P. Syngas Suitability for Solid Oxide Fuel Cells Applications Produced via Biomass Steam Gasification Process: Experimental and Modeling Analysis. *J. Power Sources* **2011**, *196*, 10038–10049. [[CrossRef](#)]
14. Liu, M.; Aravind, P.V.; Woudstra, T.; Cobas, V.R.M.; Verkooijen, A.H.M. Development of an Integrated Gasifier–Solid Oxide Fuel Cell Test System: A Detailed System Study. *J. Power Sources* **2011**, *196*, 7277–7289. [[CrossRef](#)]
15. Omosun, A.O.; Bauen, A.; Brandon, N.P.; Adjiman, C.S.; Hart, D. Modelling System Efficiencies and Costs of Two Biomass-Fuelled SOFC Systems. *J. Power Sources* **2004**, *131*, 96–106. [[CrossRef](#)]
16. Athanasiou, C.; Coutelieris, F.; Vakouftsi, E.; Skoulou, V.; Antonakou, E.; Marnellos, G.; Zabaniotou, A. From Biomass to Electricity through Integrated Gasification/SOFC System—Optimization and Energy Balance. *Int. J. Hydrogen Energy* **2007**, *32*, 337–342. [[CrossRef](#)]
17. Ouweltjes, J.P. *Report Summarising the Literature Review for Selection of Representative Syngas Compositions Including Organic and Inorganic Contaminants*; European Union Funding for Research and Innovation: Brussel, Belgium, 2019.
18. Aravind, P.V.; de Jong, W. Evaluation of High Temperature Gas Cleaning Options for Biomass Gasification Product Gas for Solid Oxide Fuel Cells. *Prog. Energy Combust. Sci.* **2012**, *38*, 737–764. [[CrossRef](#)]
19. EU UNIQUE Coprooperative Research Project, Contract N.211517 7FP. 18 January 2013. Available online: <https://cordis.europa.eu/project/id/211517/reporting> (accessed on 3 November 2021).
20. Gallifuoco, A.; Taglieri, L.; Scimia, F.; Papa, A.A.; Di Giacomo, G. New Insights into the Evolution of Solid and Liquid Phases during Hydrothermal Carbonization of Lignocellulosic Biomasses. *Biomass Bioenergy* **2019**, *121*, 122–127. [[CrossRef](#)]
21. González-Arias, J.; Sánchez, M.E.; Martínez, E.J.; Covalski, C.; Alonso-Simón, A.; González, R.; Cara-Jiménez, J. Hydrothermal Carbonization of Olive Tree Pruning as a Sustainable Way for Improving Biomass Energy Potential: Effect of Reaction Parameters on Fuel Properties. *Processes* **2020**, *8*, 1201. [[CrossRef](#)]
22. Gallucci, K.; Taglieri, L.; Papa, A.A.; Di Lauro, F.; Ahmad, Z.; Gallifuoco, A. Non-Energy Valorization of Residual Biomasses via HTC: CO<sub>2</sub> Capture onto Activated Hydrochars. *Appl. Sci.* **2020**, *10*, 1879. [[CrossRef](#)]
23. Ramke, H.-G.; Blöhse, D.; Lehmann, H.-J.; Fettig, J. Hydrothermale Carbonisierung Organischer Siedlungsabfälle. *Kern M Hrsg Bio-Sekundärrohstoffverwertung* **2010**, *22*, 141–157.
24. Hwang, I.-H.; Aoyama, H.; Matsuto, T.; Nakagishi, T.; Matsuo, T. Recovery of Solid Fuel from Municipal Solid Waste by Hydrothermal Treatment Using Subcritical Water. *Waste Manag.* **2012**, *32*, 410–416. [[CrossRef](#)] [[PubMed](#)]
25. Zhao, P.; Shen, Y.; Ge, S.; Yoshikawa, K. Energy Recycling from Sewage Sludge by Producing Solid Biofuel with Hydrothermal Carbonization. *Energy Convers. Manag.* **2014**, *78*, 815–821. [[CrossRef](#)]
26. Prawisudha, P.; Namioka, T.; Yoshikawa, K. Coal Alternative Fuel Production from Municipal Solid Wastes Employing Hydrothermal Treatment. *Appl. Energy* **2012**, *90*, 298–304. [[CrossRef](#)]
27. Lee, S.Y.; Park, S.W.; Alam, M.T.; Jeong, Y.O.; Seo, Y.-C.; Choi, H.S. Studies on the Gasification Performance of Sludge Cake Pre-Treated by Hydrothermal Carbonization. *Energies* **2020**, *13*, 1442. [[CrossRef](#)]
28. Ahmed, M.; Sartori, F.; Merzari, F.; Fiori, L.; Elagroudy, S.; Negm, M.S.; Andreottola, G. Anaerobic Degradation of Digestate Based Hydrothermal Carbonization Products in a Continuous Hybrid Fixed Bed Anaerobic Filter. *Bioresour. Technol.* **2021**, *330*, 124971. [[CrossRef](#)]
29. Funke, A.; Ziegler, F. Hydrothermal Carbonization of Biomass: A Literature Survey Focussing on Its Technical Application and Prospects. In Proceedings of the 17th, European biomass Conference; from Research to Industry and Markets; Produced and published by ETA-Florence Renewable Energies, Hamburg, Germany, 29 June–3 July 2009.
30. Papa, A.A.; Taglieri, L.; Gallifuoco, A. Hydrothermal Carbonization of Waste Biomass: An Experimental Comparison between Process Layouts. *Waste Manag.* **2020**, *114*, 72–79. [[CrossRef](#)]
31. Gerhardt, M.; Berg, M.; Kamm, B. Hydrothermal Carbonization of Lignocellulosic Biomass and Its Precursors. In Proceedings of the International Conference on Polygeneration Strategies with Special Focus on Integrated Biorefineries, Leipzig, Germany, 7–9 September 2010.
32. Torres-Mayanga, P.C.; Lachos-Perez, D.; Mudhoo, A.; Kumar, S.; Brown, A.B.; Tyufekchiev, M.; Dragone, G.; Mussatto, S.I.; Rostagno, M.A.; Timko, M.; et al. Production of Biofuel Precursors and Value-Added Chemicals from Hydrolysates Resulting from Hydrothermal Processing of Biomass: A Review. *Biomass Bioenergy* **2019**, *130*, 105397. [[CrossRef](#)]

33. Gallifuoco, A.; Taglieri, L.; Scimia, F.; Papa, A.A.; Di Giacomo, G. Hydrothermal Carbonization of Biomass: New Experimental Procedures for Improving the Industrial Processes. *Bioresour. Technol.* **2017**, *244*, 160–165. [[CrossRef](#)]
34. Lucian, M.; Piro, G.; Fiori, L. A Novel Reaction Kinetics Model for Estimating the Carbon Content into Hydrothermal Carbonization Products. *Chem. Eng. Trans.* **2018**, *65*, 379–384. [[CrossRef](#)]
35. Lucian, M.; Fiori, L. Hydrothermal Carbonization of Waste Biomass: Process Design, Modeling, Energy Efficiency and Cost Analysis. *Energies* **2017**, *10*, 211. [[CrossRef](#)]
36. Reza, M.T.; Uddin, M.H.; Lynam, J.G.; Hoekman, S.K.; Coronella, C.J. Hydrothermal Carbonization of Loblolly Pine: Reaction Chemistry and Water Balance. *Biomass Convers. Biorefinery* **2014**, *4*, 311–321. [[CrossRef](#)]
37. Becker, R.; Dorgerloh, U.; Paulke, E.; Mumme, J.; Nehls, I. Hydrothermal Carbonization of Biomass: Major Organic Components of the Aqueous Phase. *Chem. Eng. Technol.* **2014**, *37*, 511–518. [[CrossRef](#)]
38. Mutlu, Ö.Ç.; Zeng, T. Challenges and Opportunities of Modeling Biomass Gasification in Aspen Plus: A Review. *Chem. Eng. Technol.* **2020**, *43*, 1674–1689. [[CrossRef](#)]
39. Rapagnà, S.; Gallucci, K.; Foscolo, P.U. Olivine, Dolomite and Ceramic Filters in One Vessel to Produce Clean Gas from Biomass. *Waste Manag.* **2018**, *71*, 792–800. [[CrossRef](#)] [[PubMed](#)]
40. Savuto, E.; Di Carlo, A.; Steele, A.; Heidenreich, S.; Gallucci, K.; Rapagnà, S. Syngas Conditioning by Ceramic Filter Candles Filled with Catalyst Pellets and Placed inside the Freeboard of a Fluidized Bed Steam Gasifier. *Fuel Process. Technol.* **2019**, *191*, 44–53. [[CrossRef](#)]
41. Fercher, E.; Hofbauer, H.; Fleck, T.; Rauch, R.; Veronik, G. Two Years Experience with the FICFB-Gasification Process. In Proceedings of the 10th European Conference and Technology Exhibition, Wurzburg, Germany, 8–11 June 1998; pp. 3–6.
42. Moradi, R.; Carlo, A.D.; Testa, F.; Zotto, L.D.; Bocci, E.; Habib, E. Comparison between 1-D and Grey-Box Models of a SOFC. *E3S Web Conf.* **2019**, *128*, 01007. [[CrossRef](#)]
43. Pérez-Fortes, M.; Nguyen, T. System Models Considering Component Operating Windows and Plant Chp Operating Scenarios. *Zenodo* **2020**. [[CrossRef](#)]
44. *Perry's Chemical Engineers' Handbook*, 8th ed.; Perry, R.H.; Green, D.W. (Eds.) McGraw-Hill: New York, NY, USA, 2008; ISBN 978-0-07-142294-9.
45. Salaudeen, S.A.; Acharya, B.; Dutta, A. Steam Gasification of Hydrochar Derived from Hydrothermal Carbonization of Fruit Wastes. *Renew. Energy* **2021**, *171*, 582–591. [[CrossRef](#)]
46. Zhao, P.; Shen, Y.; Ge, S.; Chen, Z.; Yoshikawa, K. Clean Solid Biofuel Production from High Moisture Content Waste Biomass Employing Hydrothermal Treatment. *Appl. Energy* **2014**, *131*, 345–367. [[CrossRef](#)]
47. Román, S.; Nabais, J.M.V.; Laginhas, C.; Ledesma, B.; González, J.F. Hydrothermal Carbonization as an Effective Way of Densifying the Energy Content of Biomass. *Fuel Process. Technol.* **2012**, *103*, 78–83. [[CrossRef](#)]
48. He, C.; Tang, C.; Li, C.; Yuan, J.; Tran, K.-Q.; Bach, Q.-V.; Qiu, R.; Yang, Y. Wet Torrefaction of Biomass for High Quality Solid Fuel Production: A Review. *Renew. Sustain. Energy Rev.* **2018**, *91*, 259–271. [[CrossRef](#)]
49. Gallifuoco, A.; Taglieri, L.; Scimia, F.; Papa, A.A.; Di Giacomo, G. Hydrothermal Conversions of Waste Biomass: Assessment of Kinetic Models Using Liquid-Phase Electrical Conductivity Measurements. *Waste Manag.* **2018**, *77*, 586–592. [[CrossRef](#)] [[PubMed](#)]